OPTIMIZATION OF THE FABRICATION PARAMETERS FOR SERS-ACTIVE FORENSIC EVIDENCE SWABS

A thesis presented to the faculty of the Graduate School of Western Carolina University in partial fulfillment of the requirements for the degree of Masters of Science in Chemistry.

By

Katarina Grace Perrine

Advisor: Dr. David D. Evanoff, Jr.
Associate Professor of Chemistry
Department of Chemistry & Physics

Committee Members: Dr. Scott Huffman, Chemistry & Physics
Dr. Kelly Grisedale, Forensic Science
Mrs. Brittania Bintz, Forensic Science

April 2018

ACKNOWLEDGEMENTS

First and foremost I would like to thank my advisor, Dr. Evanoff for his consistent dedication and guidance throughout this project. I will be forever grateful for his enthusiasm and commitment toward broadening my knowledge and skills as a chemist. I would like to thank my committee members, for their time and continued support with not only this project but any other questions I might have agitated them with. Specifically Britt Bintz for guidance with all DNA trials and for performing the experiments depicted in Figures 16 & 18. I would like to give a special thanks to other members of the chemistry department that have supported me through my time at Western. Specifically Dr. Carmen Huffman, for giving exceptional guidance throughout my time as a graduate student. James Cook and Wes Bintz for all of the behind-the-scenes engineering and fixing of various things for this project.

I would like to thank my husband, Lucas Perrine, for his constant support and confidence in my abilities, even in my wavering self-doubt. I would like to thank my parents for their overwhelming support and their monumental example of dedication set forth as recipients of graduate degrees. I would also like to thank all the friends that have helped me endure not only graduate school but my entire five-year journey at Western Carolina. Lastly, I would like to thank the National Institute of Justice for helping to fund this project (2015-NE-BX-K003).

TABLE OF CONTENTS

LIST OF TABLES

LIST OF FIGURES

LIST OF ABBREVIATIONS

DTT	Dithiothreitol
HBF	Human bodily fluid
NR	Normal Raman spectroscopy
PCR	Polymerase chain reaction
PSA	Prostate-specific antigen
$Ru[bpy_3]^{+2}$	Tris(2,2'-bipyridyl)ruthenium(II) chloride
SERS	Surface enhanced Raman spectroscopy
SORS	Spatial offset Raman Spectroscopy

ABSTRACT

OPTIMIZATION OF THE FABRICATION PARAMETERS FOR SERS-ACTIVE FORENSIC EVIDENCE SWABS

Katarina Grace Perrine, Masters of Science in Chemistry

Western Carolina University (April 2018)

Advisor: Dr. David D. Evanoff, Jr.

Currently, in the forensic field there is a need for development to improve biological evidence screening. Although, biological evidence screening is not required for DNA analysis it can give insight for crime scene reconstruction therefore providing valuable forensic evidence.[1] Many current screening tests have several limitations such as low specificity, lack of sensitivity and sample destruction.[1] The proposed research introduces a method to collect and identify body fluid that is not only reliable but non-destructive to the sample. This can be achieved by fabrication of SERS-active forensic swabs via a silver nanoparticle synthesis. The modified swabs allow for rapid sample identification via surfaced enhance Raman spectroscopy. Several studies were performed to further enhance the synthesis reaction. A multi-point Raman measurement method was developed for Raman intensity comparison between varying synthesis conditions. Surface coverage of swab fibers and total mass of silver on swabs was also analyzed. A synthesis reaction at 80 °C for 90 minutes was found to be the optimal parameters however, additional research may be needed to confirm these results. Lastly, the effects of silver contamination on DNA extraction and quantification were assessed. It was also concluded that the SERS-active forensic evidence swabs performed just as well as plain swabs when used for DNA extraction and quantification.

CHAPTER ONE: BACKGROUND

Current Forensic Techniques for Identification of Human Bodily Fluids

Today, in the forensic field, there are a variety of tests that are used to screen for human bodily fluids (HBF) such as blood, seminal fluid, saliva, etc. The confirmatory identification of human bodily fluids is often a prerequisite for analysis of DNA from forensic evidence, which can be crucial in criminal court cases. Although biological evidence screening is not needed for DNA analysis, it can give insight as to the nature of a crime. The origin and type of body fluid found at a crime scene can potentially support the link between the sample donor and a criminal act.[1] Therefore, biological screening can be imperative to a criminal investigation.[2] However, current screening tests can be time consuming, body-fluid specific, and prone to false positive and negative results.[3] In addition, advances in DNA profiling have lead to a low limit of detection that has surpassed that of many screening tests.[4]

Presumptive Tests

Presumptive and confirmatory evidence screening tests are performed before DNA analysis. Since human bodily fluids can be either invisible to the naked eye or give the same appearance as another bodily fluid it can be difficult to determine the type of bodily fluid or even if there is one present.[5] Presumptive tests aim to solve one of these problems by indicating the presence of a particular bodily fluid. Although these tests may give the type of biological sample they do not specify between species of the given sample. There are several presumptive tests, per bodily fluid, that are actively employed in the forensic field and forensic laboratories. Generally, presumptive tests for blood utilize the peroxidase-like activity of the heme group in hemoglobin.[4] Some tests are chemical, such as luminol, which when oxidized emits light. Luminol oxidation is catalyzed when a metal ion is present. In the case of blood, heme in hemoglobin contains iron that catalyzes the oxidation thus luminescing the sample for the visual identification of blood. Compared to other tests, luminol has high sensitivity and specificity between body fluid types.[1]

However, it may give false positives in the presence of other metal containing compounds and has the potential to effect subsequent DNA analysis.[1] Other tests use a chemical color change such as the Kastle-Meyer test. The Kastle-Meyer test also uses heme to promote the oxidation of phenolphthalein which causes the sample to turn pink when in the presence of blood.

For seminal fluid screening, presumptive tests historically relied on the forensic analyst to observe stains only based on appearance and consistency. Currently, the acid phosphatase color test (AP) has been favorable to initially differentiate seminal fluid from other bodily fluids.[6] Considering the acid phosphatase concentration found in semen is 400 times the amount found in any other human bodily fluid, it is a useful compound for determining the presence of semen.[6] The acid phosphatase color test involves moistening filter paper, and dabbing it over the suspected area for absorption of suspected seminal fluid. A solution of α-napthylphosphate and Fast Blue dye is then added. In the presence of acid phosphatase, hydrolysis of α-naphthyl phosphate produces α-napthol which couples with diazonium to form a purple colored precipitate acting as the identification for the presence of semen.[6] Although effective and widely used, there are downfalls to using acid phosphatase for seminal fluid identification, such as false positives for solutions also containing high concentrations of acid phosphatase. These solutions include but are not limited to certain fruits and vegetables, contraceptive creams, and vaginal fluid.[6] However, none of these solutions react to the SAP test as quickly as seminal fluid, therefore, if the reaction occurs in less than 30 seconds there is a strong indication of seminal fluid.[6]

Each of the presumptive tests listed above are human bodily fluid specific, therefore they require the analyst to have prior knowledge as to the identity of the fluid before choosing an appropriate presumptive test. If the wrong test is chosen, a portion of the sample most likely has been destroyed, thus destroying DNA evidence and another test must be performed. In addition, presumptive tests are only used for initial detection therefore further confirmation may still be needed. In addition, further testing may be needed to specify the species or gender of the sample to determine if it may be useful as evidence.

Confirmatory Tests

Confirmatory tests should not only confirm the identity but also provide the species of a body fluid. For some bodily fluids such as blood and saliva, confirmatory tests are commonly not performed.[4] However, the Takayama test can be used for the confirmation of blood by a precipitation reaction. The Takayama tests relies on a series of reactions with hemoglobin to produce hemochromogen in the form of pink crystals. However, these crystals may be difficult to obtain therefore a negative result does not necessarily confirm the absence of blood.[4]

Confirmatory tests for seminal fluid may involve the microscopic identification of spermatozoa by immersing the stain in water and stirring to transfer sperm cells into solution. A stain test is then needed, such as the Christmas Tree Stain test, to stain the neck and tail sections of the sperm cells. A drop is then dried onto a microscope slide and examined with a 400x objective.[6] The probability of locating sperm cells from seminal fluid is large because of the naturally high concentration of sperm cells in seminal fluid samples. However, there are multiple complications that may occur using this technique. The Christmas Tree Stain test can be damaging to DNA therefore, it may yield poor DNA results.[4] Spermatozoa can become extremely brittle when dry therefore causing the sample to disintegrate.[6] The sample can also be disrupted if it is washed or comes into contact with any other objects.[6] Additionally, spermatozoa may not be present in the sample because the male donor may have (1) a low sperm count (oligospermia), (2) the absence of sperm (aspermia), or (3) have had a vasectomy. If any of these problems arise another test can be done to detect a protein called the prostate-specific antigen (PSA). PSA, also referred to as p30, can be detectable through many methods, a few common ones with sensitive detection are, the ABAcard® p30 test and the BioSign™ p30 membrane test kit.[4]

Emerging Techniques

Considering the need for development of an improved body fluid screening technique there have been recent developments that offer potential solutions. One emerging technique involves the use of biosensors called quantum dots that are well-known for detection of molecules in a wide

range of applications.[7] Quantum dots are semiconducting materials made as nano-structures so that they may be embedded into biological molecules for various applications. When mixed with blood their unique optical properties gave the characteristic fluorescence spectra with no degradation to DNA.[8] Although this method has high specificity and sensitivity there has been little research conducted on the use of quantum dots for bodily fluid identification.[7]

Another developing technique, involving the extraction of mRNA, can be used for single bodily fluid sample identification and bodily fluid mixtures. This study introduces a method where mRNA and DNA are co-isolated to enable identification of bodily fluid type and DNA profiling from a signal extraction.[9] For the identification of seminal fluid, Alvarez et al. found that, in samples as low as 0.2 μL, mRNA could be used to detect protamine 1, a protein found in semen, to confirm identification. In addition, the DNA fraction yielded complete STR profiles for identification.[9] Spectroscopic techniques such as Raman Spectroscopy and Fourier transform infrared spectroscopy (FTIR) have also been studied because of their ability to give structural information of biological molecules and frequent use for identification of other substances.[7]

Raman Spectroscopy

Raman Spectroscopy in Forensic Science

Raman spectroscopy is a rapidly growing technique in the field of forensic research because of its ability to provide unique spectra based on vibrational modes of the material's molecules.[10] Raman spectroscopy has become a useful analytical technique because it allows for little to no sample preparation and is generally nondestructive.[11] Although Raman has proven to be a useful technique, its applications still remain in research laboratories. Several groups are assessing the use of Raman spectroscopy for the identification of fibers,[12] inks,[13] drugs,[14] explosives,[15] and automotive paints.[16] DeGelder et al. explored the use of Raman spectroscopy for the identification of automotive paints. Collection of spectroscopic information for each layer of a given paint can reveal the manufacturer of the car in question. DeGelder et al. discovered that paints were easily distinguished by Raman measurements of the base-coat. This method not only proved to be effec-

tive but also efficient considering there was little to no sample preparation.[16] Another application of Raman spectroscopy in forensic science involves the identification of liquid explosives in various containers. This can be a difficult task considering the unstable nature of the sample, however, Eliasson et al. used a Raman technique called spatial offset Raman spectroscopy (SORS). This technique allowed for identification of the sample without fluorescence interference from the sample container.[15]

The ability to identify various human body fluids has also been performed using Raman spectroscopy. Bodily fluid samples were placed on aluminum foil covered microscope slides and measured with a 785 nm laser line at a power of 115 mW at the sample.[10] Lednev et al. has used this Raman method to differentiate between blood, saliva, sweat, seminal fluid, and vaginal fluid. In addition, they have also shown Raman spectroscopy can be used for the differentiation between species and body fluid mixtures.[5] Although many advancements, there is still much development needed in this research. Interferences in Raman may occur depending on the substrate to which the sample is adhered. At a crime scene there is an immeasurable amount of different substrates where a sample may exist. In addition, a high powered laser is used for this research which may cause DNA damage. Further research is needed to prove that this technique is sufficient for forensic workflow.

Theory of Raman Spectroscopy

Raman spectroscopy is a vibrational spectroscopic technique that measures the interaction between light and matter by scattered light. Scattered light can be described by two different types, Rayleigh scattering and Raman scattering. Rayleigh scattering is an elastic interaction where the scattered light is at the same energy and frequency as the incident electromagnetic field. Raman scattering is an inelastic interaction that occurs when there is a change in the molecule's vibrational energy by the incident light. Stokes and Anti-stokes Raman are two different scattering processes in which a change in a molecule's vibrational energy occurs. Stokes Raman occurs when a photon interacts with a molecule's ground state electron and excites it to a higher energy

virtual state. When a molecule relaxes back to the ground electronic state and the photon is scattered, some of the photon's energy is retained by the molecule, increasing the vibrational evergy state of the molecule and decreasing the frequency of the scattered light with respect to the incident radiation (shown in Figure 1). In Anti-stokes Raman, a molecule in an excited vibrational state is excited to a virtual state and transfers energy to the photon during relaxation, lowering the molecule's vibrational state and increasing the frequency of the scattered radiation with respect to the incident radiation. The amount of energy exchanged can depend on the vibrational modes of the given molecule. The number of vibrational modes can be calculated by the following equation:

$$n = 3N - 6 \tag{1}$$

where n_l is vibrational modes and N is number of atoms. Vibrational modes can be IR-active, Raman-active or both. A molecule's vibrations can be IR-active when the molecule experiences a change in dipole moment. Infrared bands are observed when the molecule's oscillating dipole occurs at the same frequency as the incident infrared radiation. For a molecule to be Raman-active it must experience a change in polarizability. Polarizability is the ability of a molecule's electron cloud to become distorted by an incident electromagnetic field. This interaction can also be described using the equation below,

$$\mu = \alpha E \tag{2}$$

where μ is the induced dipole moment, α is the polarizability, and E is the incident electric field.[17]

Another Raman scattering process, called Resonance Raman, is more favorable than the typical Stokes and Anti-stokes interaction leading to a signal enhancement on the order of 10^3 or 10^4.[18] Resonance Raman occurs when the molecule's oscillating dipoles are at the same frequency as the incident electromagnetic field. As shown in Figure 1, Resonance Raman is similar

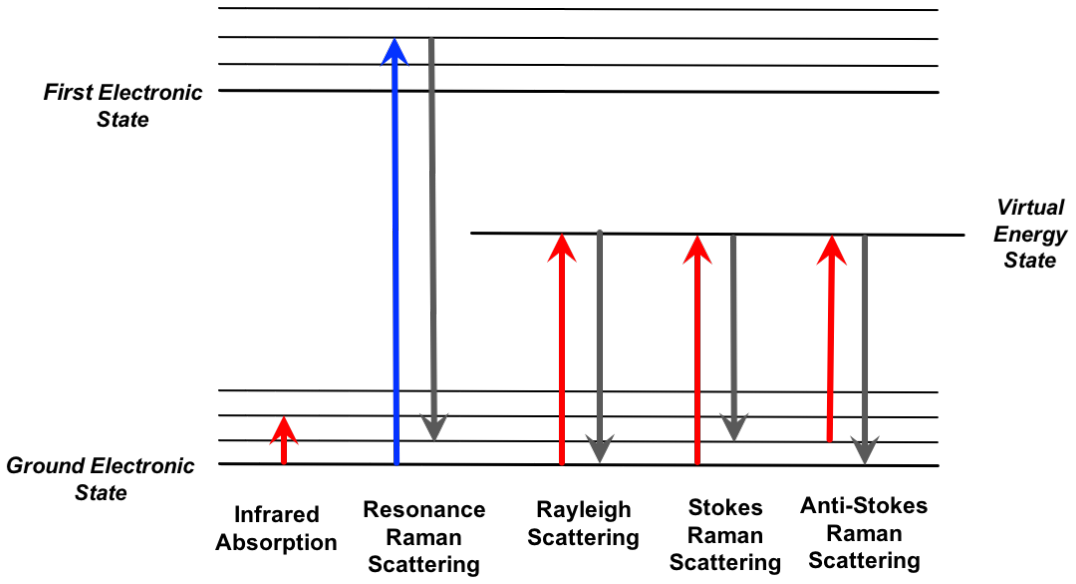

Figure 1. Jablonski diagram showing infrared absorption and various forms of scattered light.

to Stokes Raman except the molecule's electron is excited to the first electronic state instead of a virtual state. As a result of this resonant excitation, fluorescence is less likely to interfere with Raman signal because, in this process, fluorescence is less probable than Raman scattering.

Surface Enhanced Raman Spectroscopy

Surface Enhanced Raman Spectroscopy in Forensic Science

Surface enhanced Raman Spectroscopy (SERS) became popular in the early 1980s because of it versatility in many fields of study.[19] In forensic research, SERS has been used for identification of a variety of sample types including the identification of various ink dyes. Geiman et al. reported that ink dyes were identifiable using normal Raman (NR) spectroscopy if the appropriate excitation frequency had been chosen. In contrast, they found that when using SERS their resulting spectra consistently contained enhanced, fluorescent quenching signal.[13] Rana et al. compared normal Raman spectral data to SERS spectral data for the identification of controlled substances including morphine, codeine, and hydrocodone. They were able to identify the controlled substances using normal Raman by performing spectral manipulation to eliminate fluo-

rescence interferences, which resulted in the introduction of artifacts into the data.[20] However, they reported that resulting SERS spectra had heavily enhanced signal with naturally quenched fluorescence signal.[20]

Theory of Surface Enhance Raman Spectroscopy

SERS is a technique that heavily enhances the intensity of scattered light by the use of metal nanoparticles to enhance the analyte's signal through interactions of the metal's plasmon resonances with the molecule's electronic structure. Common metals used are silver, gold and copper because they possess plasmon resonances in the visible spectrum.[21] These metal nanoparticles have a unique ability to react with light at an extremely high efficiency.[21] Ag nano-structures interact with light so well that they capture more light than incident on them.[21] Plasmon resonances that occur in noble-metal nanoparticles are the collective oscillation of the particle's conduction electrons, represented in Figure 2a, which oscillate at the same frequency as the incident light.[21] Depending on the size of the particle, frequencies of electromagnetic radiation may cause multiple forms of plasmon resonances. In the case of a 100 nm diameter silver particle, 500 nm radiation causes a dipole resonance in which the electron oscillates parallel to the axis of the electric field of the incident light. 420 nm radiation causes excitation of a quadrupole resonance in 100 nm particles, as depicted in 2b (B), with oscillations both parallel and perpendicular to the incident electric field. 380 nm radiation causes excitation of an octupole resonance in 100 nm silver nanoparticles, as shown in Figure 2b (C). The oscillation of electrons, which can last for approximately 5-50 fs following excitation, create an oscillating, non-propagating local electromagnetic field that extends from the particle's surface a distance approximately equal to its radius.[22] Therefore, when sample molecules are placed near a nano-material surface its local electromagnetic field increases the analyte molecule's susceptibility to changes in polarizability increasing the probability of Raman scattering by the analyte molecule 10^6 to 10^{14} times, a mechanism termed electromagnetic enhancement.[21] If the sample molecule is deposited directly onto a metal nanoparticle, Raman scattering may also be increased by another mechanism termed chemical

enhancement. In chemical enhancement a 'hot electron' is transferred to the analyte molecule during the particle's plasmon resonance. The injected electron affects the molecule's polarizability, increasing the Raman cross-section of the molecule by a factor of 10^4 to 10^6. These two enhancement processes operate independently of each other however, when they can be applied to the same system the effects are multiplicative.[23]

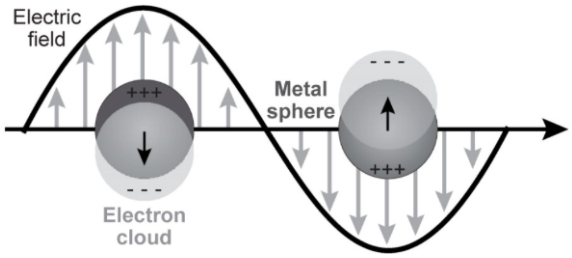

(a) Diagram depicting the plasmon resonance that occurs when shining monochromatic light onto metal nanoparticles.[24]

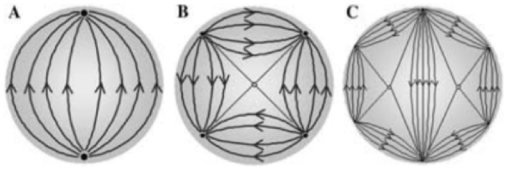

(b) The oscilation patterns of elctrons depending on the incident electric field: (A) dipole, (B) quadrupole, and (C) octapole.[21]

Figure 2. The excitation of a nanoparticle's conduction electrons so that they may oscillate at the same frequency as incident light (left) and the patterns at which they may oscillate (right)

Introduction to Research

The overall purpose of this research is to develop a nonspecific, one-step method that is more rapid, cost-effective, and reliable than current serological screening methods. This is achieved by adhering silver nanoparticles to forensic evidence swab fibers creating a SERS-active substrate where, once collected, human bodily fluids may be rapidly identified using Raman spectroscopy. A fabrication method had been previously developed and proven to be effective for identification of seminal fluid.[25] It was found that synthesized SERS-active swabs could be used to obtain a viable Raman spectrum of semen from as little as 12 µL of sample.[25] The specific goal of the project presented here was to study the effect of swab fabrication parameters on SERS enhance-

ment and on downstream STR typing of DNA extracted from seminal fluid. Various trials were conducted including (1) a reaction time study, (2) a reaction temperature study, and (3) a study of the effects of silver on a commercially available DNA extraction method. The reaction time study involved changing the reaction time of the silver nanoparticle synthesis followed by the assessment of the Raman signal produced by a model compound. The reaction temperature study varied the temperature silver nanoparticle synthesis and assessed the amount of silver grown on the swabs, and the ability of the silver-modified swabs to enhance the Raman signal of a model compound. The final trial consisted of quantifying the amount of silver before, during, and after DNA extraction protocol while using swabs prepared with varying reaction temperatures. The affect of silver on downstream DNA analysis was studied because of the potential silver interference in current DNA extraction and PCR techniques. The PrepFiler extraction kit uses magnetic particles to facilitate reversible binding of DNA and allow DNA to remain bound throughout wash steps.[26] The magnetic particles allow DNA to bind to their surface via phsico-chemical interactions.[26] Silver particles and or silver ions may have the potential to interfere with this process. In addition silver has been shown to cause inhibition in PCR. Yang et al. observed that silver nano-materials bind to genomic DNA which, could cause potential inhibition in PCR.[27] Further analysis was needed to determine if the SERS-active swabs would cause interference with DNA extraction and or PCR.

CHAPTER TWO: EXPERIMENTAL

Materials

Nanoparticle Synthesis, Swabbing and DNA Extaction

The nylon swabs used in this research were Copan FLOQswabs™ acquired from Life Technologies™. The silver (I) oxide (99%) was acquired from Strem Chemicals and the silver nitrate (99%) from Fisher Scientific. Hydrogen gas (research grade, 99.9995%) was acquired from Airgas. Ultrapure water was always obtained from a Barnstead NANOpure Diamond system with a 0.2 μm hollow fiber filter, at a measured resistivity of 18.2 MΩ-cm. Falcon® conical tubes used for storage were acquired from Fisher Scientific. The 5000 mL heavy wall Pyrex vessel was obtained from Ace Glass Inc. Tris(2,2'-bipyridyl)ruthenium(II) chloride (98%) was acquired from Acros Organics. 0.45 μm nylon syringe filters from Fisher Scientific were used for swab fiber filtering in silver quantification analysis. An Applied Biosystems™ PrepFiler™ Forensic DNA Extraction Kit was used for silver analysis and DNA quantification.

Instrumentation

A Horiba LabRAM HR Raman microscope with an 1800 groove/mm grating, an 800 mm monochromator, and a TE-cooled charge-coupled device (CCD) detector was used for all SERS measurements. In addition, SERS measurements were done using a 10x objective, a neutral density filter of 1.0 with a power of 0.100 W (0.5 mW to 0.8 mW at the sample) at a 1 second acquisition time and 10 accumulations. LabSpec 6 software was used to autofocus before each measurement, with range and step varying per sample. The 457.9 nm excitation from a Spectra Physics 2065-7S Ar+ laser was used for all $Ru[bpy_3]^{+2}$ samples. Additionally, a Helium-Neon 632.8 nm wavelength laser was used for all samples containing seminal fluid. A Perkin Elmer Optima 4100DV inductively-coupled plasma optical emission spectrometer (ICP-OES) was used to quantify silver on the swabs before, during and after DNA extraction protocol. To image silver coverage on the nylon swab fibers, a Hitachi SU6600 scanning electron microscope (SEM) was used.

Methods

Fabrication of Silver-Coated Evidence Swabs

The hydrogen reduction method was used for silver nanoparticle synthesis.[21] This method allows for the slow growth of pure silver nanoparticles at a suitable size for efficient light interaction resulting in significant light scattering.[21] The synthesis reaction equation for this method is as follows,

$$Ag_2O(aq) + H_2(g) \longrightarrow 2\,Ag^0(s) + H_2O(l) \tag{3}$$

where solid silver (I) oxide in excess is immersed in water, heated to desired temperature, and pressurized with 10 psi of hydrogen gas. This reduces the silver oxide to allow for the pure growth of silver nanoparticles. First, the swab applicators were cut in half to allow for consistent movement while stirring the synthesis. Without this step the swabs will cluster around the thermometer. As a pre-reaction treatment, nylon swabs were soaked in ultrapure water for 24 hours followed by a aqueous saturated silver oxide soak for another 24 hours. The saturated silver oxide solution was prepared by gravity filtration of ultrapure water and silver (I) oxide, using 0.2 micron filter paper. After a thorough cleaning of the reaction vessel, it was filled with approximately three liters of ultrapure water. Pre-treated swabs were added and 2.5 g of silver (I) oxide were added along with a PTFE-coated egg-shaped stir bar. The reaction vessel was then placed in a heating mantle and set to stir at 700 rpm and heat to the desired temperature. To better equilibrate the heating temperature, the vessel was pressurized with nitrogen gas at 10 psi to simulate the hydrogen gas pressurization. Once the reaction vessel equilibrated to the desired temperature the nitrogen gas was released. The vessel was then flushed with 5 psi of hydrogen gas three times, and a final pressure was set to 10 psi. Once the reaction was set to 10 psi of hydrogen gas, reaction time was started. Each synthesis reaction was allowed to procede for 90 minutes unless specifically stated otherwise. After 90 minutes, the hydrogen gas was released from the vessel

and stirring and heating were stopped. The vessel and its contents were allowed to cool until safe to handle. The swabs were then removed from suspension and rinsed with ultrapure water. Prepared SERS-active swabs were stored, five at a time, in 50 mL conical tubes containing ultrapure water until needed for analysis.

Raman Spectroscopy Measurements

For Raman spectroscopy measurements, swabs were removed from ultrapure water and were dried in conical tubes with Kimwipe™ coverings. For accelerated drying time, the swabs were stored in a desiccator. For analysis of swab efficiency, a 10^{-4} M $Ru[bpy_3]^{+2}$ solution was used as the analyte for Raman measurements. Approximately 180 µL of $Ru[bpy_3]^{+2}$ solution was pipetted onto a hydrophobic substrate and collected with silver-modified swabs. The swabs were then dried using the method previously described. Once the $Ru[bpy_3]^{+2}$ solution had dried, swabs were mounted on a microscope slide by taping the applicator to the slide to avoid movement during measurement. The 457.9 nm argon ion laser was used for all samples containing $Ru[bpy_3]^{+2}$. The laser was always aligned by measuring a silicon standard and ensuring that the 520 cm^{-1} band of the silicon Raman spectrum was greater than or equal to 6,000 cps. Once the laser was aligned, the X and Y dimensions of each swab were recorded by simply moving the stage in the x and y direction. Similarly a z (focal) range was found by focusing in and out on the swab fibers. As depicted in Figure 3, 9 points were measured in a 3x3 grid to acquire a diverse range of spectra from the swab face. Before each measurement was collected the instrument automatically focused on the swab fiber along the z axis to maximize Raman signal. All measurements were taken with a one second acquisition time and 10 accumulations. The power at the sample ranged from 0.5 mW to 0.8 mW depending on the measurement. During data analysis all 9 points were averaged together to produce a single spectrum per swab. For each synthesis condition, such as different reaction temperatures, five swabs were measured. To eliminate variation from swab to swab the five swabs measured were averaged to obtain one spectrum for each condition. All data analysis including averaging spectra was performed in Origin 2017 software. Once a spectrum

was obtained for each condition an Asymmetric Least Squares baseline correction was completed and the resulting spectra was over-layed for comparison. Integration of the 1488 cm^{-1} band of the $Ru[bpy_3]^{+2}$ spectrum was also completed using Origin 2017. A data range from 1437 cm^{-1} to 1526 cm^{-1} was used along with an end-point weighted baseline correction and a gaussian band model for integration.

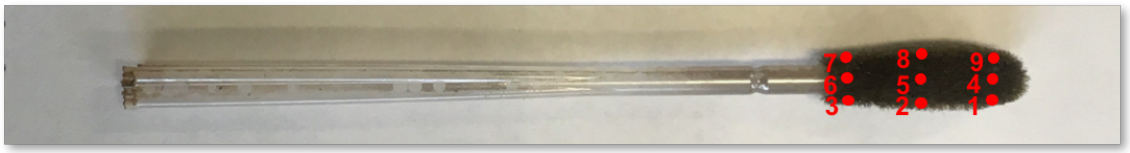

Figure 3. A SERS-active forensic swab showing the grid of 9 points that are measured on each swab. Points 1-9 are labeled in the order they are measured.

Silver Quantification

ICP-OES analysis was performed to analyze the effect of reaction temperature on quantity of silver grown. Standards were prepared with concentrations ranging from 10 ppb to 10 ppm. Initially, 100 mL of a 500 ppm stock solution was prepared by dissolving approximately 0.787 g of $AgNO_3$ in the solvent of choice, 10% nitric acid. A serial dilution was performed to obtain all 7 standard concentrations. The silver-modified swabs used were made with 6 different reaction temperatures: 60 °C, 70 °C, 80 °C, 90 °C, 100 °C, and 110 °C. Three swabs per temperature were used for this analysis. First, the swab heads were cut from the applicators and placed in individual 15 mL conical tubes where 2.00 mL of concentrated nitric acid was added. The swabs were sonicated for 20 minutes to ensure all silver particles had dissolved in solution. The samples were diluted to 20% nitric acid by adding 8 mL of ultrapure water. To remove the swab fibers from solution, each sample was filtered with 0.45 μm nylon syringe filters. The samples were then diluted to 10% nitric acid. Silver concentrations were calculated using data collected from the Ag 328.068 nm and Ag 338.289 nm wavelengths.

DNA Extraction

To assess the effects of synthesis temperature on amount of silver leached in the lysis step, three swabs from each temperature, 60 °C, 70 °C, 80 °C, 90 °C, 100 °C and, 110 °C were used. Each swab was placed in its own 1.5 mL eppendorf tube and labeled. 300 µL of PrepFiler™ Lysis Buffer was added to each sample along with 5 µL of 1.0 M dithiothreitol (DTT). The samples were briefly vortexed (1-2 seconds) and centrifuged (15 seconds) then placed in a thermal shaker, heated to 70 °C for 90 minutes at 900 rpm. The PrepFiler™ extraction protocol suggests that solid substrate be removed by incorporating an extra centrifuge step following incubation. Each swab was removed using tweezers and placed in a PrepFiler™ filter column which was then placed back into the original centrifuge tube. The samples were centrifuged for 2 minutes at 13,400 rpm. The swabs were then transferred to clean eppendorf tubes and the filter columns were discarded. The remaining contents in the original centrifuge tubes contained the lysis buffer mixture and now a pellet of solid silver that had collected at the bottom. The lysis buffer supernatant was aspirated by pipetting and transferred into new eppendorf tubes.

The amount of silver present (1) on the swabs, (2) in the buffer solutions, and (3) in the silver pellets was quantified using ICP-OES. Silver standards were produced by first making 100 mL of an approximately 500 ppm stock solution. The stock solution was made by weighing approximately 0.787 g of $AgNO_3$ and adding to a 100 mL volumetric flask. The flask was then filled with 10% nitric acid solution. The stock solution was then used to make standards with concentrations varying from ca. 10 ppb to 10 ppm. The swab sample preparation was the same as previously discussed in *Silver Quantification* section on page 14 except that the solutions required additional 10-fold dilutions to fall within the standard concentration range. For buffer sample preparation, 305 µL was transferred into 15 mL conical tubes. To obtain 5 mL of sample diluted to 10% nitric acid, 0.5 mL of concentrated nitric acid was added along with 4.195 mL of ultrapure water. Lastly, the silver pellet samples were prepared by adding 1 mL of concentrated nitric acid to the sample eppendorf tubes followed by a brief vortex to dissolve all of the silver stuck

at the bottom of the tubes. The samples were then pipetted into new 15 mL conical tubes and diluted to 10% nitric acid by adding 9 mL of ultrapure water. An additional 10-fold dilution were performed as needed to ensure the sample concentrations would fall within the concentration range of standards.

Another trial was performed to quantify the amount of silver in purified DNA extracts. The second trial began with the same samples, three swabs per temperature. During this study the entire protocol for the PrepFiler™ Forensic DNA Extraction Kit was used. As was the case in the trial described above, no human bodily fluid or DNA was used in this study. The method in this study for cell lysis, as described above, was completed. After this step however, the resulting solution, known as the sample lysate, was carried forward to the DNA binding step of the extraction protocol. 15 µL of the PrepFiler® Magnetic Particle suspension was pipetted into each sample lysate, then they were set to vortex at low speed for 10 seconds and centrifuged for 15 seconds. Additionally, 180 µL of isopropanol was added to each tube and the the samples were, again, vortexed for 1-2 seconds and centrifuged for 15 seconds. The sample lysate tubes were then placed in a thermal shaker for incubation at room temperature for 10 minutes while stirring at 1,000 rpm. Step 5 of the PrepFiler™ Forensic DNA Extraction kit is intended to wash DNA. In this step the samples were vortexed at 10,000 rpm for 10 seconds, centrifuged for 15 seconds and then placed in a magnetic stand for approximately two minutes. According to the protocol, for the following steps, each wash buffer should be discarded. However, the spent wash buffers were transferred to new tubes and stored to be analyzed later for silver content. While the samples remained in the magnetic stand, all liquid contents were carefully pipetted into a new set of eppendorf tubes. The remaining magnetic particles were then washed via three separate wash steps. First, 600 µL of Wash Buffer A was pipetted into the magnetic particle samples then they were vortexed for five seconds at 10,000 rpm and centrifuged for 15 seconds. The samples were placed back in the magnetic stand for about a minute then the wash buffer was carefully removed and transferred into new eppendorf tubes. Then the same wash process was completed two more

times except with 300 µL of Wash Buffer A followed by 300 µL of Wash Buffer B. After the removal of the last wash buffer, the magnetic particles were allowed to dry for 10 minutes. Finally, elution was completed by adding 50 µL of PrepFiler® Elution Buffer. Samples were then vortexed at 10,000 rpm for five seconds and centrifuged for 15 seconds. The sample tubes were placed in the thermal shaker for five minutes at 70 °C and 900 rpm. After incubation, samples were vortexed for 1-2 seconds and centrifuged for 15 seconds to remove any magnetic particle pellets from the side of the tubes. Lastly, the tubes were placed in the magnetic stand until the magnetic particles pelleted. The remaining eluate was removed and saved for elemental analysis.

CHAPTER THREE: RESULTS AND DISCUSSION

Raman Spectroscopy Spatial Point Analysis

Because the work in this project was to determine, at least semi-quantitively, the effect of varying swab parameters on SERS signal, a standard operating procedure to measure SERS signal on forensic evidence swabs was developed. In previous efforts in our lab, the goal had been simply to obtain viable Raman data to prove the success for the initial fabrication method, therefore the variation in Raman intensities on a single swab or between multiple swabs had not yet been studied (refer to Figure 4b). Not only is Raman scattering an improbable occurrence that is often difficult to reproduce but the swab fibers and the orientation of silver nanoparticles on them is not uniform, thus allowing for great variation from measurement to measurement.

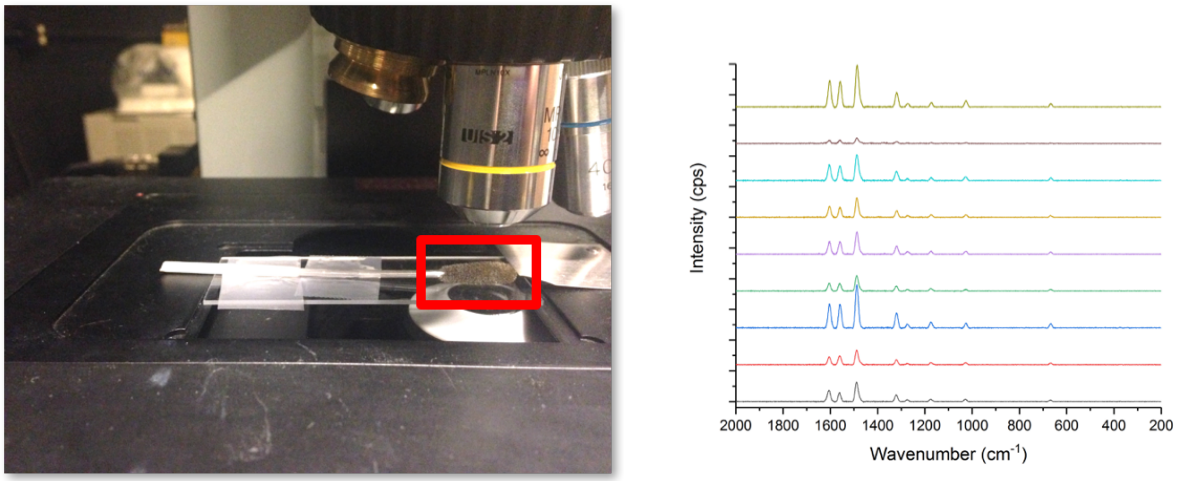

(a) A swab mounted and aligned for Raman measurements.

(b) Nine different Raman spectra measured on one swab with the spatial analysis technique.

Figure 4. A picture of a swab under the Raman microscope (left) and the resulting 9 spectra from one 9-point analysis.

For a successful comparison of Raman spectra, a spatial 9-point analysis previously described on

page 13 was developed. This method involved a feature in the LabSpec 6 software that allowed for multiple points on a swab face to be sequentially analyzed during a single measurement cycle. A 9-point 3x3 grid of measurements was chosen in order to collect spectra from the tip, middle, applicator-end, and both sides of a swab face to determine the average spectral response across the swab. First, the swab was mounted on a microscope slide by taping the applicator down. Then the slide is placed underneath the Raman microscope as shown in Figure 4a. The size of the grid is determined by the individual dimensions of each swab therefore, the edges in the x and y dimensions are found by adjusting the stage in video mode to determine the edges of the swab head. Once the x and y dimensions are found the center of the swab is calculated and all dimensions are inputted into the appropriate table under the acquisition tab in the LabSpec 6 program. An appropriate z range is then found by focusing in and out on the middle and edges of the sample. The z range (focal depth) is applied to the auto-focus function so that the software records the maximum Raman signal once the spectral focal plane is found. The nine spectra obtained from a swab varied in intensity, as seen in Figure 4b, and were averaged together to give a resulting spectrum for each swab. However, previous research had shown that the silver nanoparticle growth on the swab fibers is also somewhat inconsistent. To compensate for variation in different swabs, five swabs from each condition were measured with the 9-point spatial analysis. Each of the five resulting spectra were averaged together to obtain one spectrum for that condition. For example, in determining the representative SERS spectrum for swabs fabricated at 80 °C, 5 swabs with the same amount of $Ru[bpy_3]^{+2}$ deposited were analyzed in 9 different locations with 10 accumulations averaged at each location such that each representative spectrum is the average of 450 individual measurements.

While 9-point analysis was used for the remainder of this study, some basic statistical analysis was completed to assess the value of this multi-point analysis. Using the 9-point average as the 'true value', the root mean square error of each possible combination of few-point averages was calculated. For example, the root mean square error of each of the possible 126 combinations

of 5 point averages was calculated and plotted as a box and whisker plot as shown in Figure 5. As expected, the mean and median values of the error decay towards zero as more measurement locations are added to the average. Likewise, quartile boxes decrease in size as the spectral averages approach the same value. However, what is apparent in the figure is that a full 9 points of data per swab may not be necessary to obtain a representative average.

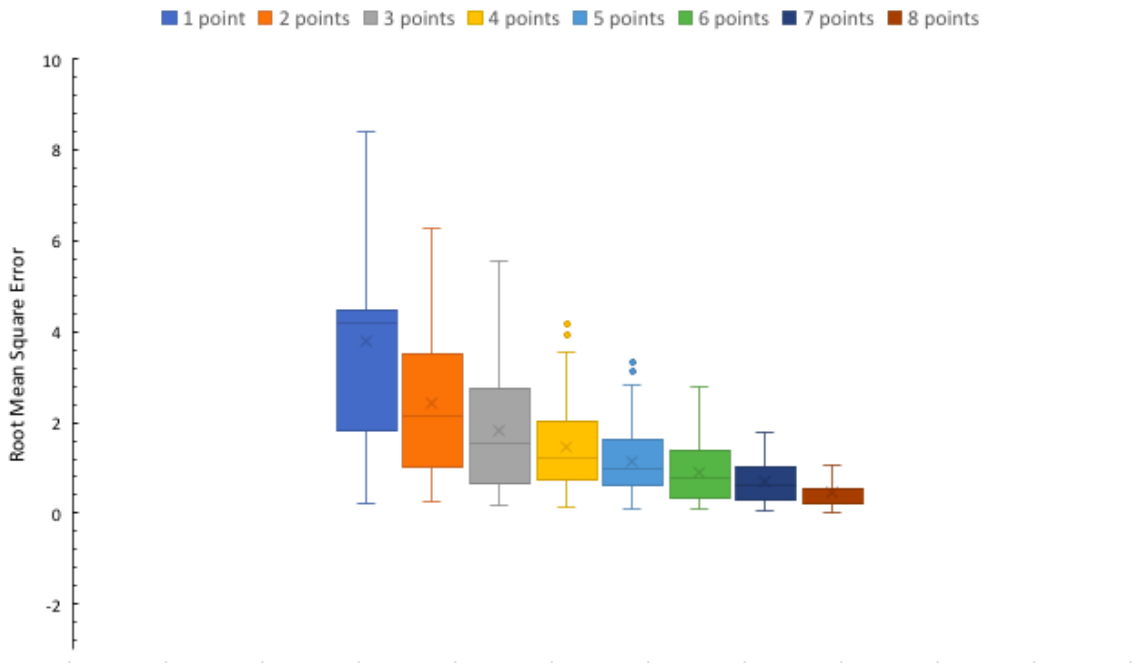

Figure 5. Box an whisker plot of the root mean square averages of each multi-point analysis compared to a 9-point average.

Above an average of three points, the root mean square errors are quite similar and may not add much information. In Figure 5, the average of the root mean square errors is normalized by the seconds of acquisition time needed to make the measurement. While the full 9 point acquisition requires around 15 minutes, Figure 6 shows that there is a clear 'diminishing return' in the error reduction as more data is collected on a particular swab. While further study is still needed to de-

termine the minimum number of points that should be interrogated on a particular swab, Figures 5 and 6 would seem to suggest that four or five points is likely sufficient. There is certainly cause for further study into the need for multiple point analysis, especially into the variation from swab to swab within the same reaction conditions. However, for the purpose of this project the Raman measurements were consistently taken using a 9-point measurement.

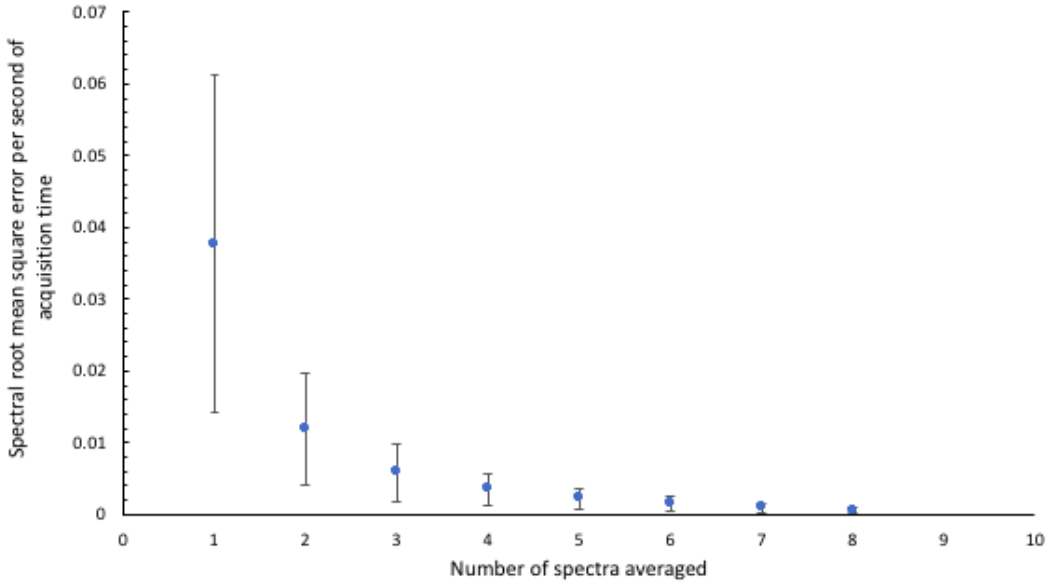

Figure 6. Root mean square averages of 1 through 8-point measurements per time taken for the measurement to occur. The error bars represent the standard deviation in the root mean square averages.

Another statistical analysis was conducted to assess the both the intra-swab and inter-swab variation in a given synthesis reaction condition. Figure 7 shows box and whisker plots of the integrated intensities of the 1488 cm^{-1} $Ru[bpy_3]^{+2}$ band at each of the 9 measurement points for five different swabs with the same synthesis reaction conditions. Although more study is needed to assess the reliability of measurements, this data is promising in that each swab produced a relatively consistent average SERS signal with respect to the amount of $Ru[bpy_3]^{+2}$ on a given swab.

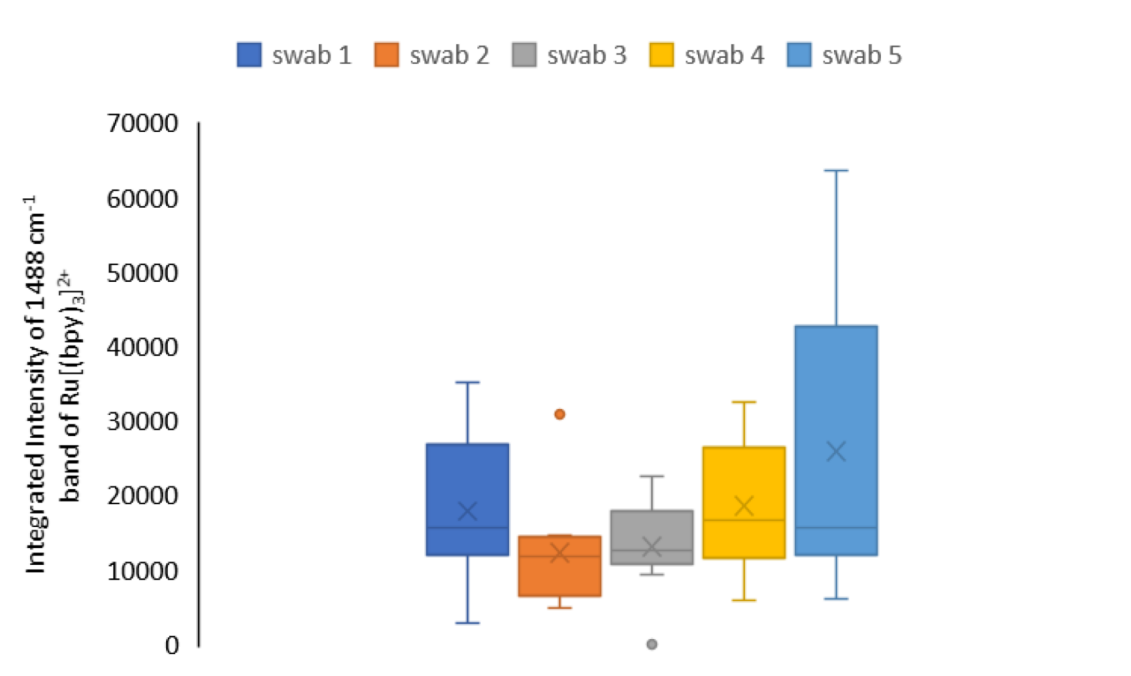

Figure 7. Spread of the intra swab variation in Raman intensities of the 1488 cm^{-1} $Ru[bpy_3]^{+2}$ band.

Reaction Time Study

As a result of using the hydrogen reduction method for silver nanoparticle synthesis, the particles exhibit a slow-growth where the size of nanoparticles can grow larger than alternative techniques.[21] Resulting nanoparticle size range from ten to above 200 nm and can be controlled via the reaction time.[21] The effects of reaction time on the how nanoparticles interact with the swab fibers was studied since nanoparticle size proportionally correlates with synthesis reaction time. Previously, the reaction time had been set at 2.5 hours to sufficiently grow nanoparticles on the swab fibers. It was found that simply stirring the reaction could drastically increase the efficiency of silver growth. Therefore, additional study on the effect of time on the deposition of silver on the swab fibers was needed. Reaction times of 0.5, 1.0, 1.5, and 2.0 hours. With this study the 9-point Raman analysis had been developed, however, only one swab per time was analyzed to

obtain Raman spectra. It was not until later studies had been performed that the 5-swab measurement technique was implemented. As previously mentioned on page 13 each swab had been used to absorb approximately 180 µL of 10^{-4} M $Ru[bpy_3]^{+2}$ solution. After fully dried, Raman spectra was collected from the swab using the 457.9 nm line of an argon ion laser.

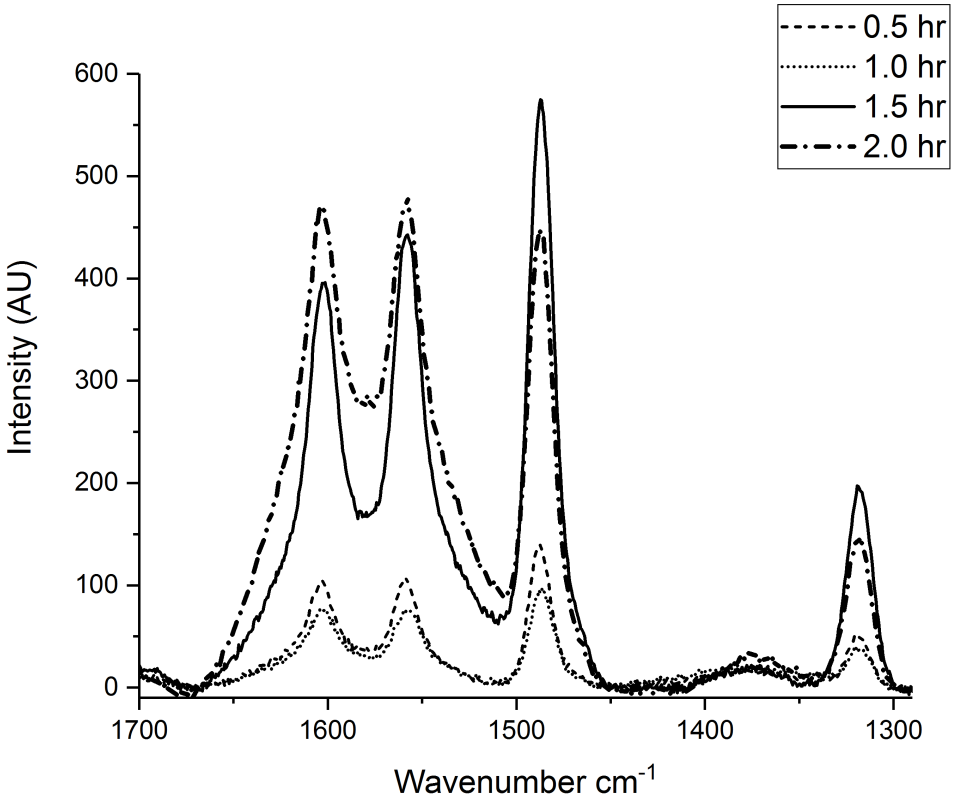

Figure 8. Raman spectral data centered at 1488 cm^{-1} for each of the reaction times analyzed: 0.5, 1, 1.5, and 2 hours.

As seen in Figure 8, the resulting spectra for each reaction time were overlaid for comparison. For a more quantitative comparison, the most prominent $Ru[bpy_3]^{+2}$ band, 1488 cm^{-1}, area was calculated using Origin 2017 software from OriginLab (Table 1). The swabs fabricated using a

Table 1. The integrated intensity of the 1488 cm^{-1} band for each time tested.

Time of Synthesis (hr)	Area Under the Curve
0.5	1,291 $\pm$ 300
1.0	939 $\pm$ 225
1.5	5,510 $\pm$ 1,579
2.0	3,657 $\pm$ 893

1.5 hour reaction time presented with the largest comparable 1488 cm^{-1} Raman intensity and area under the curve. It is important to note that the 2 hour reaction time yielded a lower Raman peak intensity than the 1.5 hour. A possible explanation for this observation is that as synthesis time progresses, the number and size of silver particles on the swabs increase.[21] To maximize SERS response, it is important that the size and spacing of particles maximize the opportunity for analyte molecules to be both in the interstitial spaces between particles and within the local electromagnetic field of those particles. In the early stages of synthesis time, particles are not yet large enough to have local electromagnetic fields that extend reasonable distances from the particle surface.[22] Likewise, the spacing between particles is, on average, quite large. At long reaction times, the particles likely become too close and are essentially fused, not allowing molecules into those interstitial spaces.

Reaction Temperature Study

The following study involved varying the reaction synthesis temperature from 60 °C to 110 °C as previously described on Page 14. A more extensive approach was taken with this study by performing not only Raman measurements but analysis by electron microscopy and silver quantification. To discuss the potential positive or negative effects that the change in temperature had on the swabs, the change in appearance must first be considered. A visual representation of the SERS-active forensic evidence swabs prepared at each temperature, along with a plain swab, is shown in Figure 9. Additionally, Figure 10 allows for closer observation of the change in color

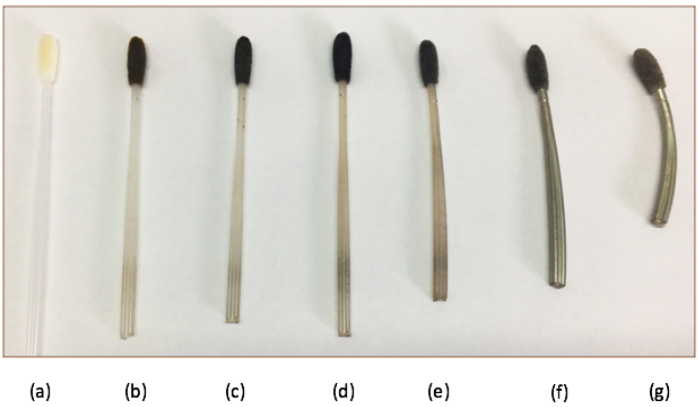

Figure 9. (a) unmodified swab and swabs modified by varying reaction temperatures: (a) is a plain swab, (b) 60 °C, (c) 70 °C, (d) 80 °C, (e) 90 °C, and (f) 100 °C, (g) 110 °C.

and texture of each individual swab. The swab fibers range in color from yellow to black, then to silver. Even though the swab prepared at 60 °C is black in color, the shade of color appears lighter in comparison to swabs prepared at 70 °C and 80 °C. The 70 °C and 80 °C swabs seem into increase in darkness as a result in the increase in temperature. However, the 90 °C through 110 °C swabs appear increasingly silver in color, which would seem to indicate that at these reaction temperatures, the average overall thickness of silver on the swab fibers is larger than the skin depth of silver. Skin depth is a measure of how far incident light travels into a particle before it is reflected back. Skin depth depends on the type of material, particle size, and the frequency of incident light. Therefore if a silver particle has grown to a size that is larger than the skin depth of silver, light is no longer traveling into the particle but is reflecting off the surface. The color changes seem to be closely related to the 'firmness' of each swab which can be attributed to the alterations occurring on the swab fibers. The fibers of swabs fabricated between 60 °C and 80 °C have a noticeable increase in the 'firmness,' observed when pressing the swab against a flat surface. The swabs fabricated between 90 °C through 110 °C exhibit this same effect, only more dramatically. Swab fabrication at higher temperatures also seem to alter the structure of the swab

itself, as can be seen in Figure 9 (applicator deformation) and Figure 10 (swab head alteration in 110 °C).

The swabs described above were also analyzed using a scanning electron microscope to visually compare the silver nanoparticle surface coverage on the swab fibers. As shown in Figure 11, the electron micrographs give a clear representation of the silver (shown in white) adhering to the surface of the nylon swab fibers. It is clear that as the synthesis temperature increases there is a drastic increase in silver surface coverage. Figure 11 shows that on the 60 °C swabs there is very little silver deposited on the fibers. However, in the electron micrograph of the 100 °C swab fibers, it appears that a majority of each swab fiber was covered in silver particles in a more smooth and consistent manner. As described previously, maximizing SERS enhancement requires a consistent and 'rough' coverage of silver across the swab fibers. The 60 °C appears to have too little silver to reliably provide SERS enhancement at any point on the swab fibers, the 100 °C fibers appear to be approaching a more smooth silver surface.

To assess the SERS enhancement provided by swabs fabricated at different temperatures, the spatial point analysis technique described on page 18 was used, the results of which are shown in Figure 12. The swabs were used to collect 180 μL of 10^{-4} M $Ru[bpy_3]^{+2}$, dried, and mounted on microscope slides. Each swab was analyzed at 9 different points, all in the same spectral focal plane, with 457.9 nm excitation provided by an argon ion laser. The resulting spectra from an individual swab were averaged along with the spectra collected from four other swabs of the same condition. The final, averaged spectrum for each temperature was overlaid to compare peak intensities, seen in Figure 12. As can be seen in Table 2, which lists the integrated intensity of the 1488 cm^{-1} band, 100 °C is the fabrication temperature that provides the largest SERS enhancement.

Figure 13 shows the variation in the integrated intensities of the 1488 cm^{-1} $Ru[bpy_3]^{+2}$ band for each synthesis temperature swab set. The 1488 cm^{-1} band integrated intensities for all 45 spectra in a swab set were averaged together and plotted. The same trend in Figure 12 is shown

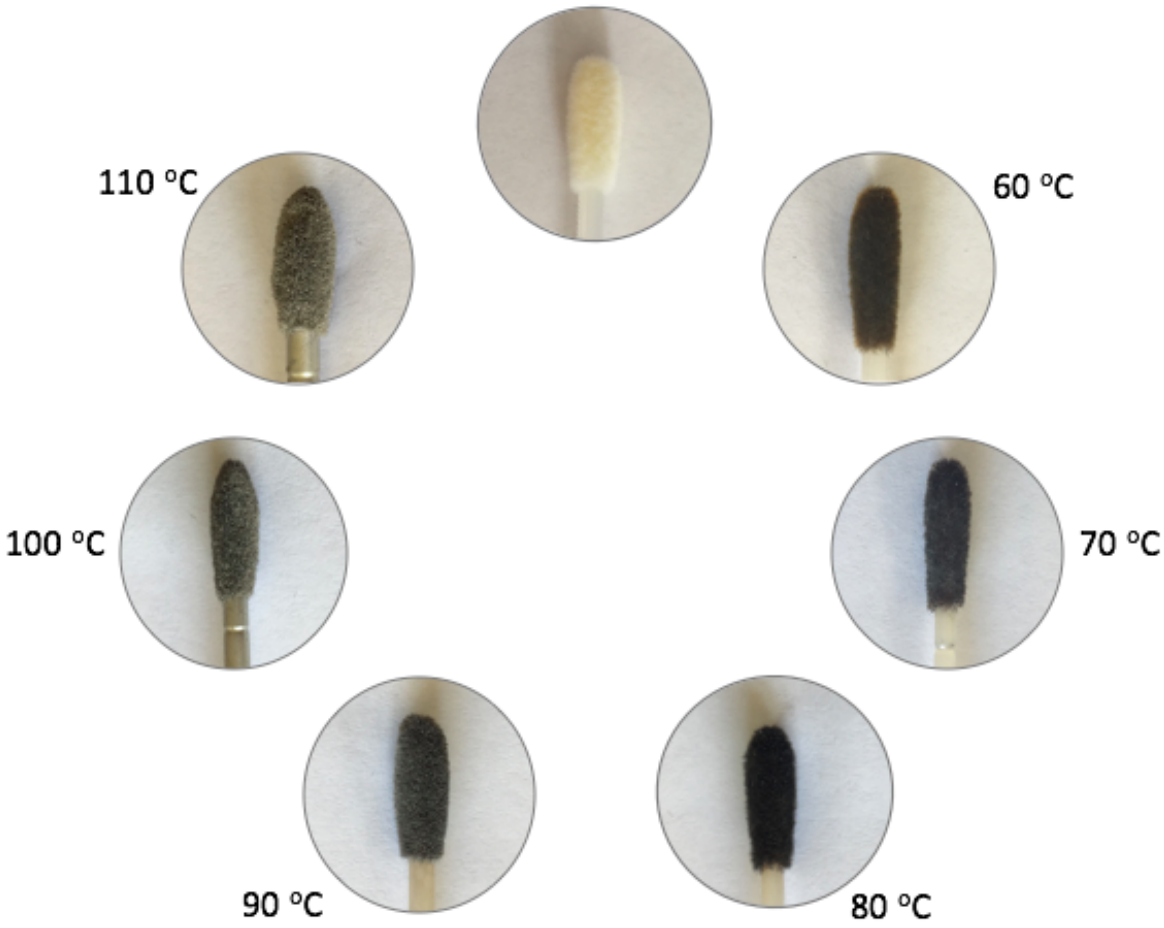

Figure 10. Close up photos of each swab head fabricated at the different temperatures, along with a plain swab head.

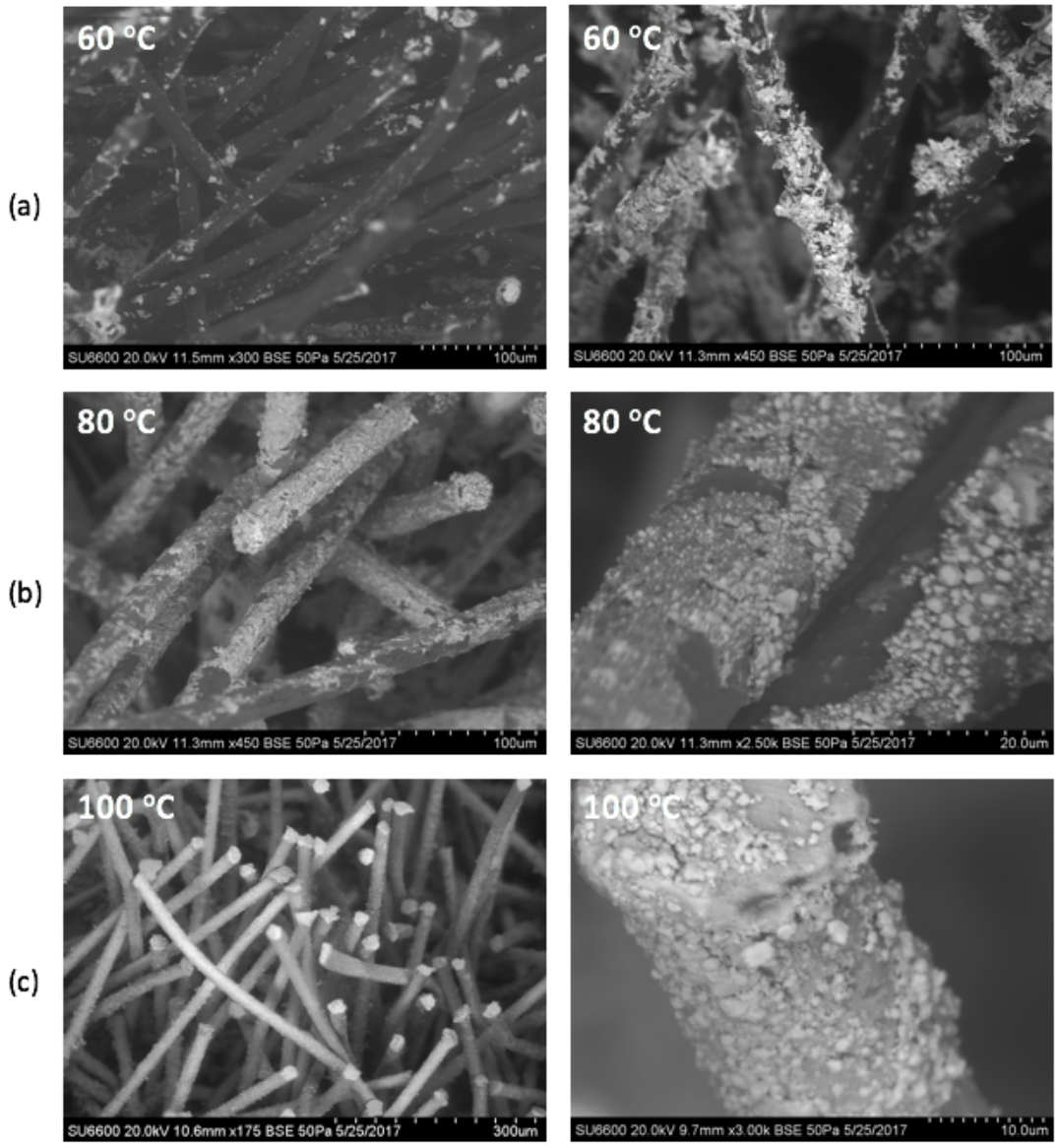

Figure 11. Electron micrographs of (a) 60 °C, (b) 80 °C, and 100 °C swab fibers. The photos on the right are zoomed in versions of the photos on the left.

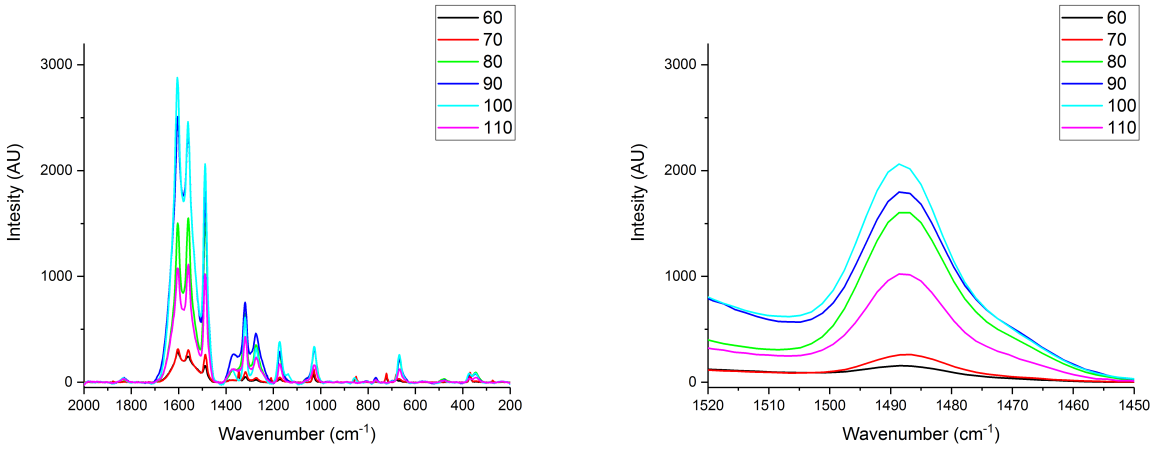

(a) The averaged spectrum resulting from each temperature overlaid.

(b) Overlaid specra showing just 1488 cm^{-1} band.

Figure 12. Averaged Raman spectra for each temperature overlaid. The entire spectrum measured (left) and the examined 1488 cm^{-1} band (right).

Table 2. Area of integrated intensities of the 1488 $^{-1}$ band for each synthesis reaction temperature spectrum.

Synthesis Temperature (°C)	Area Under the Curve
60	1,062 ± 257
70	2,355 ± 695
80	17,510 ± 2,429
90	17,561 ± 1,943
100	18,983 ± 2,193
110	7,575 ± 979

here where the 80 °C, 90 °C, and 100 °C give the highest average intensities. However, this data shows that there is still much deviation in the 45 points averaged. The outliers present are likely due to SERS hotspots which are areas that give more SERS signal than usual. This can be due to an analyte molecule existing between perfectly spaced particles. Future research is needed to assess if a there is a different data analysis method that can account for hot spots and large devia-

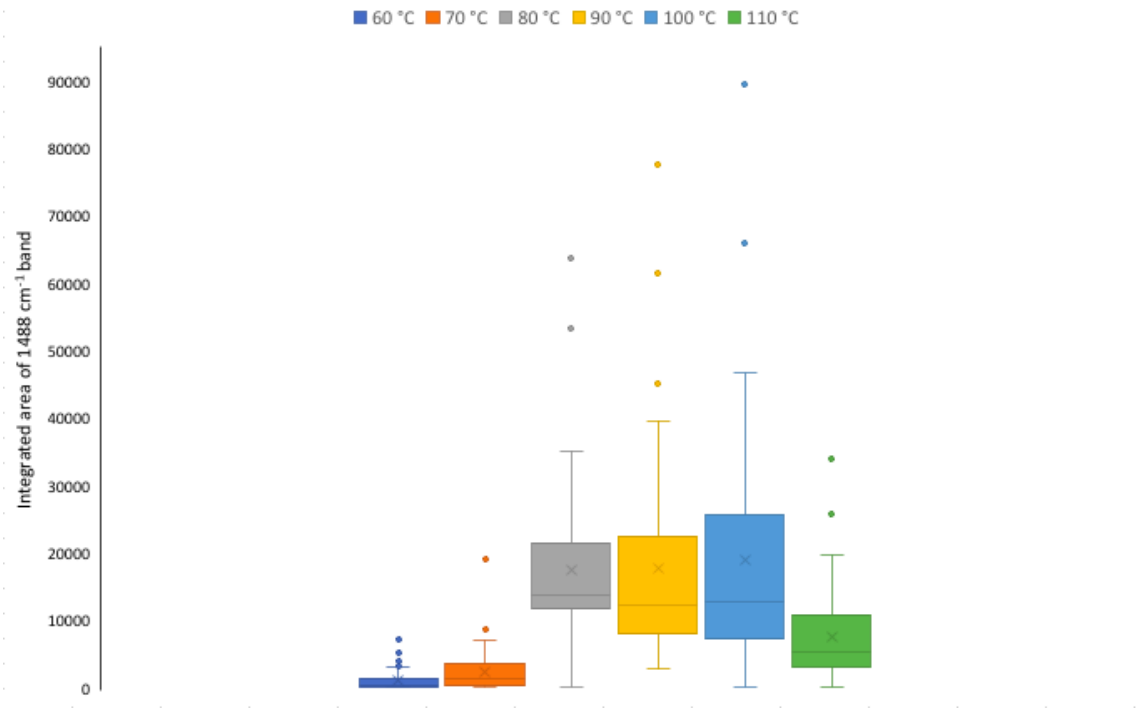

Figure 13. Box and whisker plot showing the variation is integrated area of the 1488 cm^{-1} $Ru[bpy_3]^{+2}$ band between reaction temperatures.

tion in intensity.

As described in the *Silver Quantification* section on page 14, the swabs were separated from their applicators, dissolved in concentrated nitric acid and diluted to 10% aqueous nitric acid for analysis with ICP-OES. The standard concentrations used ranged from 10 ppb to 10 ppm of silver with a 10% nitric acid solvent. The average mass of silver for each condition is shown in Table 3 followed by a visual representation in Figure 14. The 60 °C and 70 °C swabs present with the lowest amount of silver, 1.58 mg and 2.37 mg respectively, which was expected considering their appearance in color and texture (Figure 9). The 80 °C and 90 °C swabs are similar in amount of silver with 3.92 mg and 3.58 mg which can be observed as the optimal conditions. Lastly, the 100 °C and 110 °C swabs present with the largest deposition of silver on the swab with the 110 °C swabs containing 15.5 mg, a dramatic increase from the other temperatures. This upwards trend of silver mass grown on the swabs as temperature increases can be attributed to silver (I) oxide solubility. Generally, silver (I) oxide is only moderately soluble in water. At 25 °C, the solubility is reported to be 26 mg/L[28] and 53 mg/L at 80 °C.[29] As the temperature of the reaction mixture increases the concentration of dissolved silver oxide species increases and thus the rate of the reaction also increases, allowing for an increase in both silver particle number and size.

Table 3. Average mass of silver swabs for each reaction temperature.

Temperature of Synthesis (°C)	Silver on Swabs (mg)
60	1.58 ± 0.09
70	2.37 ± 0.14
80	3.92 ± 0.32
90	3.58 ± 0.22
100	5.49 ± 0.32
110	15.5 ± 0.5

To acquire a complete sense of which temperature yields the most ideal swab there are many variables to consider, such as surface coverage, Raman intensity and mass of silver. Considering Raman intensity is quantifiable via integration of a recurring prominent peak, it can be compared to amount of silver quantified. Figure 15 represents the integrated peak intensity at 1488 cm^{-1} per milligram of silver deposited on the swab with the standard error of the measurements also reported. The data presented in Figure 15 reinforces the previous assertion that there is a point at which too much silver decreases the ability for SERS to occur. Minimizing the amount of silver placed on the swabs not only keeps the fabrication cost of SERS active swabs to a minimum, it also reduces the potential effects of silver on the DNA extraction process, which will be discussed in subsequent sections. Swabs fabricated between 80 °C and 90 °C seem to produce swabs with the largest SERS enhancement for the smallest amount of silver, thus reducing cost and possible interference in the DNA extraction process.

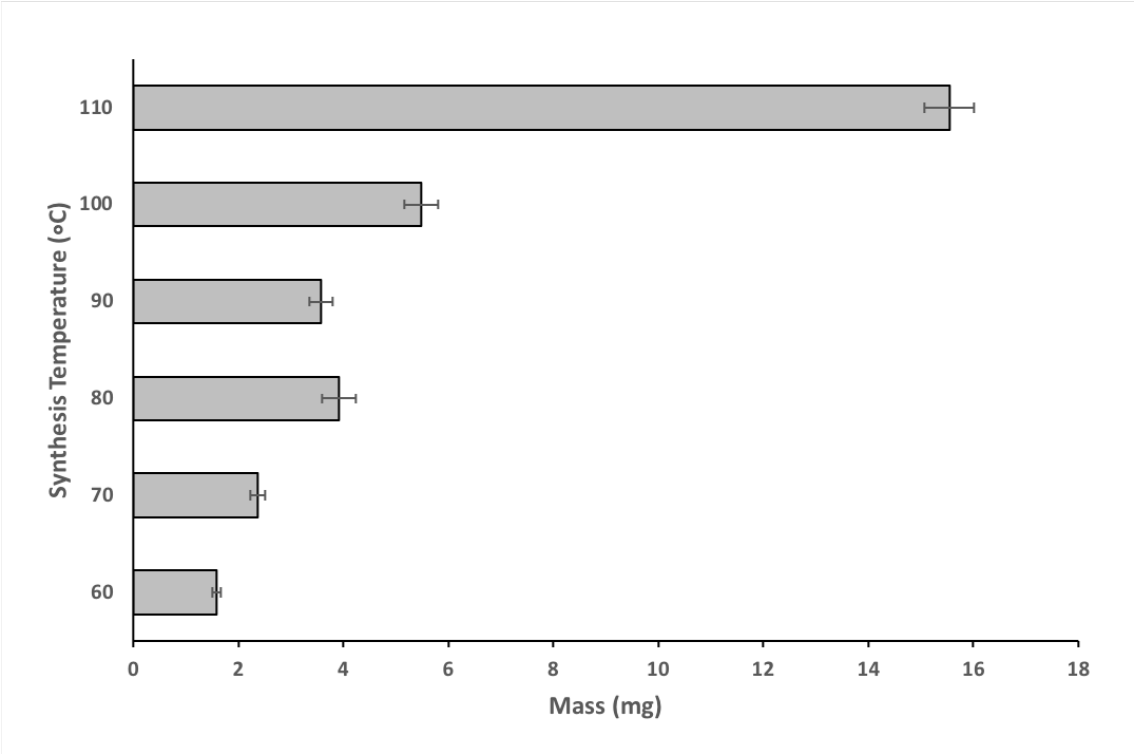

Figure 14. Visual representation of mass of silver measured for each synthesis reaction temperature.

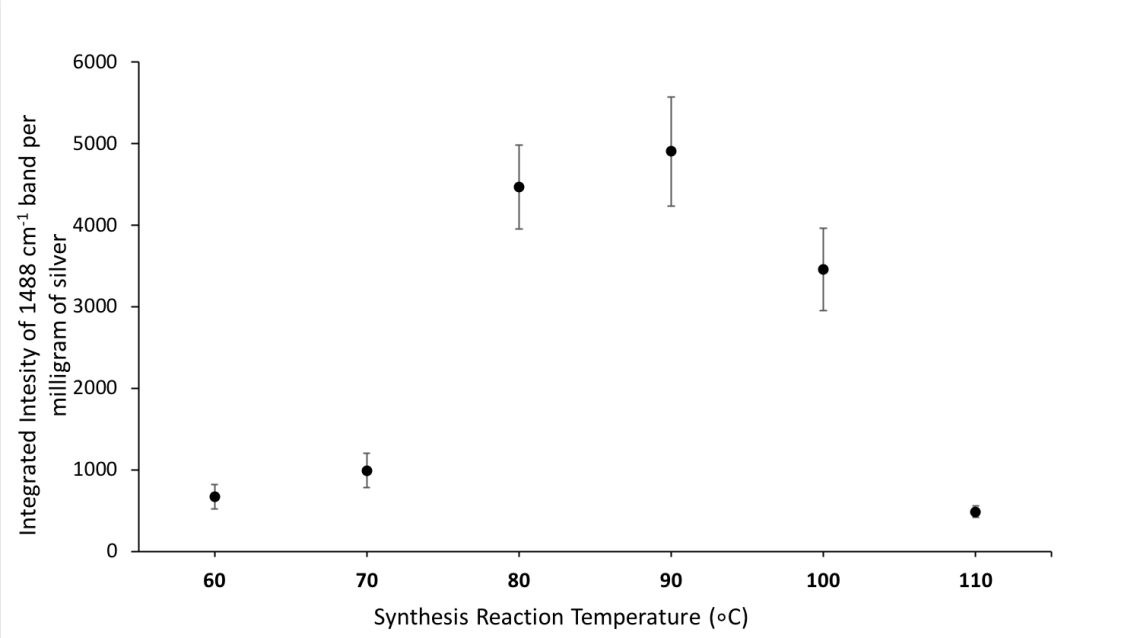

Figure 15. Plot comparing the averaged integrated intensity of 1488 $^{-1}$ peak to mass of silver found on swabs in each temperature condition.

Effect of Silver on Downstream DNA Anaysis

SERS-active forensic swabs have been shown previously to exhibit SERS enhancement of molecules such as $Ru[bpy_3]^{+2}$ and forensically relevant samples such as semen.[25] However, studies are needed to determine whether swabs have an effect on the DNA workflow downstream. To probe the effect of the silver on the DNA extraction efficiency, a study was developed that compared the extraction of known concentration of DNA doped onto plain and silver-modified swabs. The Applied Biosystems PrepFiler™ Forensic DNA Extraction Kit was used to extract DNA from the swabs. During the lysis step of extraction, it was observed that a significant amount of silver was leached from the modified swabs into the lysis buffer, essentially contaminating the lysate with silver species. Low quantities of DNA were obtained from the SERS-active swabs, as shown in Figure 16. Following extraction, purified DNA concentrations were assessed using the QuantFiler Trio DNA quantification kit form Life Technologies. This kit enables quantification of total hu-

man and total male DNA using a large autosomal (214 BP), small autosomal (80 BP), and Y chromosome target.

The low concentration of DNA on the modified swabs may be attributed to the silver species interfering with the DNA's ability to bind to the magnetic particles or the inhibition of silver in the PCR reaction. However, it is unknown as to the type of silver that may be interfering in either of these DNA analysis steps. As previously described the magnetic particles in DNA extraction bind to DNA via multiple physico-chemical interactions therefore silver ions could be interfering with this process. It is also not certain if the relatively high concentration of silver particles could be facilitating an interference. In addition, silver nanomaterial has been shown to cause inhibition in PCR.[27] Such interferences would be detrimental to the acceptance of SERS-active swabs in the forensic science community. Therefore, several studies were conducted to assess the silver species interferences in DNA extraction and DNA quantification.

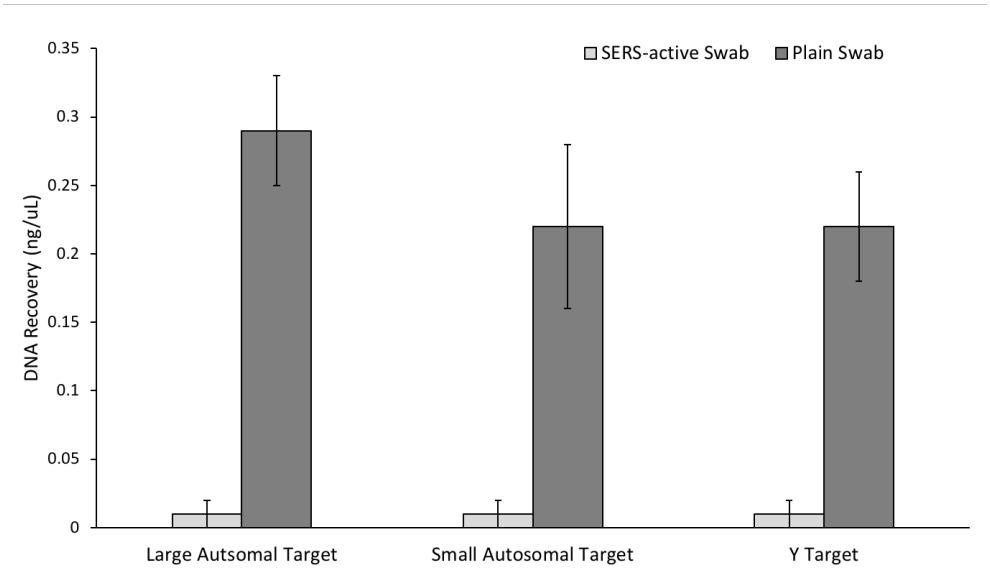

Figure 16. Quantitation of DNA with silver modified swabs and unmodified swabs.

Lysis Study

Initially, the goal of this experiment was to track the silver shed from swabs throughout DNA extraction protocol. This included analyzing the amount of silver remaining on the swabs after the lysis step, as well as the amount of silver remaining in the solutions of DNA that would continue in the DNA workflow. The appearance of swabs before, during, and after the lysis extraction step can be observed in Figure 17. In these pictures, it is apparent that the amount of silver shed from each swab is significant.

It had been hypothesized that there would be minimal to no silver in the lysis buffer supernatant after centrifugation to remove the solid substrate, since all visible solid silver appeared to be pelleted. Therefore, silver analysis was not performed past the lysis step of the DNA extraction protocol. This trial was performed by following PrepFiler™ DNA extraction protocol through Step 1:Prepare Reagents and Step 2: Perform Lysis. Three swabs per synthesis reaction temperature were used for this study. As mentioned on page 15, following lysis, the swab heads were immersed in concentrated nitric acid and the resulting silver solutions were then diluted and filtered for instrumental analysis. The pelleted silver was also dissolved in concentrated nitric acid, vortexed for 15 seconds, and diluted to 10% nitric acid. The lysis buffer was directly diluted to 10% nitric acid. All samples were analyzed with the same standard concentrations, 10 ppb to 10 ppm. Table 4 gives the average mass of silver found in each of the three mediums and their corresponding pooled standard deviations. Likewise, Table 5 presents the same data as percentages of the total amount of silver.

For swabs fabricated at 60 °C and 70 °C a large amount of visible silver appeared to leach from the surface of the swabs into the buffer solution (cf. Figure 17). However, the swabs fabricated at 80 °C to 110 °C swabs still contained a significant amount of silver, which is expected given the appearance of the swab heads after lysis and the larger initial amounts of silver on these swabs. Regardless, the data in Tables 4 and 5 indicate that the centrifugation step and subsequent supernatant transfer added after incubation is quite efficient at removing silver particles from the

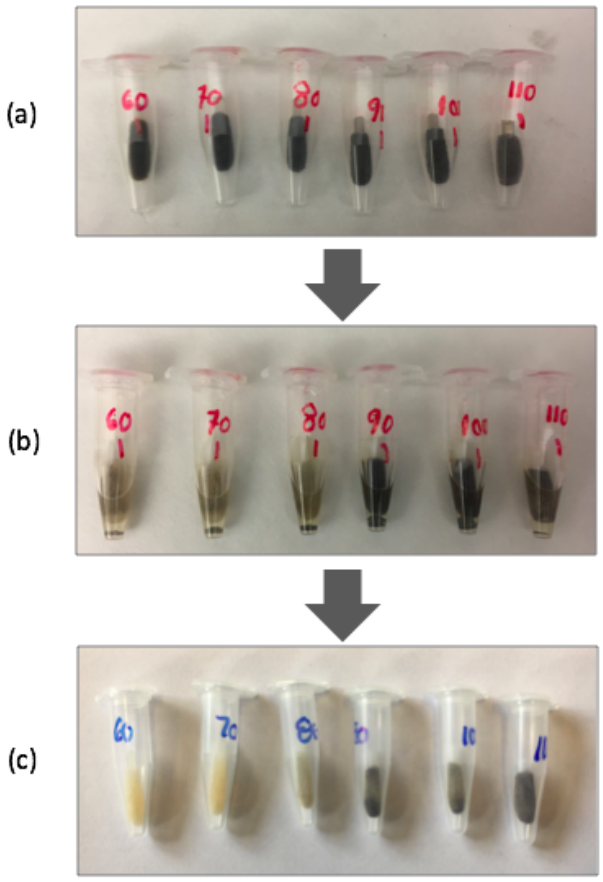

Figure 17. Photos of specific steps in the lysis protocol (a) swabs prior to lysis, (b) swabs in lysis buffer after incubation and centrifugation, and (c) swabs after removal from lysis buffer.

Table 4. Mass of silver for each of 3 mediums collected throughout the Lysis protocol: (1) swab, (2) pelletized silver, and (3) lysis buffer.

Temperature of Synthesis (°C)	Swab (μg)	Pelletized Silver (μg)	Lysis Buffer (μg)
60	35.6 ± 36.6	2060 ± 804	118 ± 78
70	8.93 ± 1.16	3120 ± 825	38.5 ± 10.7
80	8.84 ± 3.23	5000 ± 103	23.8 ± 3.1
90	502 ± 167	3300 ± 497	42.7 ± 28.7
100	381 ± 374	4070 ± 1140	30.2 ± 38.9
110	4970 ± 825	1910 ± 584	50.9 ± 49.8

lysate.

Table 5. Percentages of mass in three samples: (1) swab, (2) pellet, and (3) buffer solution.

Temperature of Synthesis (°C)	Swab (%)	Pelletized Silver (%)	Lysis Buffer (%)
60	1.60	93.1	5.32
70	0.281	98.5	1.21
80	0.176	99.3	0.475
90	13.1	85.8	1.11
100	8.49	90.8	0.674
110	71.7	27.5	0.734

Wash Step Efficiency Study

In order to asses the ability of the extraction protocol to remove the remaining silver, an experiment similar to that described above was conducted. The PrepFiler extraction protocol was carried through to completion. Multiple times in the extraction process, the beads are captured using a magnet and the remaining solution is removed and new solution is added. Generally, magnetic beads are added to the lysate to capture DNA. In this experiment, each solution removed from the magnetic beads was acidified and elemental analysis of silver was completed as described pre-

viously. With each wash step, mass of silver declines until wash 3 where it is undetectable. The amount of silver lost from step to step was not comparable between swab sets. However, the purpose of this study was to determine whether a detectable amount of silver was co-extracted with DNA that could potentially affect downstream analysis. Considering the amount of silver was undetectable by the instrument at wash 3 and the final solution there should be little silver interference in DNA results in the third wash step. In this study, 50 ppb of silver was found to the limit of quantitation, which is equivalent to 175 ng of silver in a wash. As such, a data point marked N.D. indicates that the amount of silver is no greater than 175 ng.

Table 6. Mass of silver found in each solution collected after lysis in DNA extraction.

Synthesis Temp. (°C)	Before Wash (μg)	Wash 1 (μg)	Wash 2 (μg)	Wash 3 (μg)	Final(μg)
60	39.7 ± 4.7	14.3 ± 13.5	0.542 ± 0.432	N.D	N.D
70	33.7 ± 6.4	19.0 ± 9.0	1.03 ± 0.30	N.D	N.D
80	41.6 ± 24.9	8.55 ± 1.80	1.77 ± 0.17	N.D	N.D
90	40.2 ± 18.3	23.5 ± 10.3	1.79 ± 0.35	N.D	N.D
100	30.3 ± 14.3	28.8 ± 11.9	1.61 ± 0.14	N.D	N.D
110	20.8 ± 4.04	3.34 ± 1.04	2.30 ± 0.36	N.D	N.D

DNA Extraction Quantification with Added Centrifugation

Considering the amount of silver was undetectable in the final elution buffer samples another DNA extraction was performed with the added centrifugation step. The same procedure had been used as mentioned on Page 34. As seen in Figure 18 the modified silver swabs gave DNA concentrations comparable to the plain swab DNA concentration. Thus concluding that pelletizing the silver after the lysis extraction step most likely eliminated the silver interfering with DNA extraction and DNA quantification.

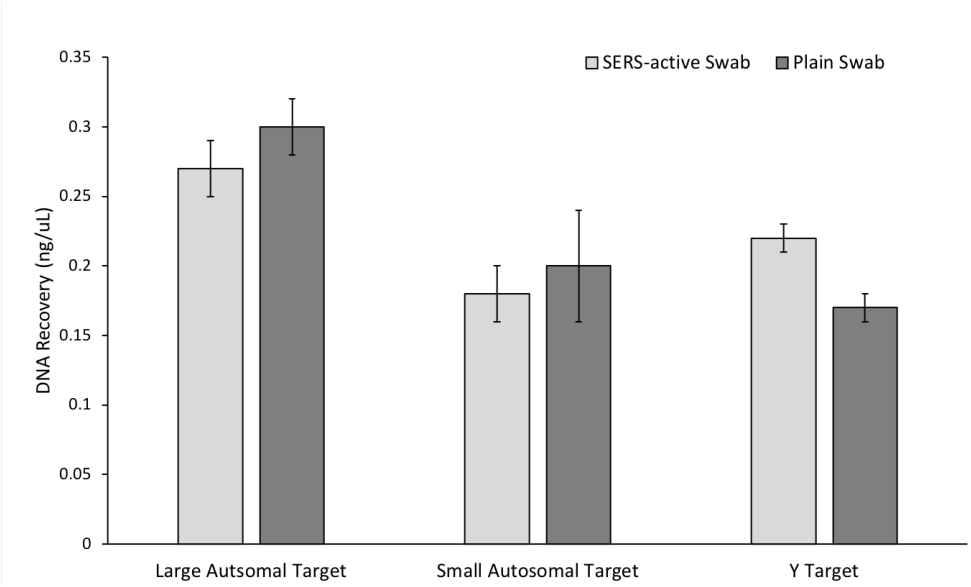

Figure 18. DNA analysis performed with an extra centrifugation step.

CHAPTER FOUR: CONCLUSIONS AND FUTURE DIRECTIONS

By developing a multi-point Raman analysis of the SERS-active swabs their resulting Raman spectra become more reliable for comparison of varying synthesis reaction conditions. A 9-point measurement however, may be excessive. The results shown in this project suggest a 4 or 5-point analysis for an individual swab would be sufficient for obtaining intensities close to the 'true value' in a shorter measurement time. However, more research and statistical analysis is needed to determine the most efficient intra-swab measurement method for Raman analysis of SERS-active forensic evidence swabs. A statistical analysis of inter-swab variation showed that measuring five swabs per synthesis reaction condition may be sufficient for synthesis reaction condition comparison. Future research should include a study involving a larger amount of points per swab and swabs per condition to further probe for an ideal measurement. The temperature study, in many ways, showed that the 80 °C synthesis reaction temperature is indeed the ideal condition. These swabs were not deformed, gave good SERS signal, were among the highest Raman intensity per mg silver and were used to successfully extract and quantify DNA as efficiently as a plain swab. As for the extraction study, more can be done to analyze the effects of silver particle vs. silver ions on extraction results. By extracting DNA with intentionally contaminated samples, results could show if and what type silver species is affecting the magnetic particle's ability to bind to DNA. Overall the studies in this project help prove that SERS-active forensic evidence swabs could be a viable confirmatory test for the screening of biological evidence. Previous work showed that seminal fluid is detectable by these modified swabs and this project showed that they do not negatively effect the currently implemented DNA extraction protocol.[25] The next steps to take should include a study of the identification of multiple types of HBFs using the silver modified swab method.

REFERENCES

[1] Rollinger, J. M. Body fluid identification in forensics. *Phytochemistry Letters* **2009**, *2*, 53–58.

[2] Kayser, M.; De Knijff, P. Improving human forensics through advances in genetics, genomics and molecular biology. *Nature Reviews Genetics* **2011**, *12*, 179–192.

[3] Virkler, K.; Lednev, I. K. Raman spectroscopic signature of semen and its potential application to forensic body fluid identification. *Forensic Science International* **2009**, *193*, 56–62.

[4] Fourney, R.; DesRoches, A.; Buckle, J. In *Interpol's Forensic Science Review*; Daeid, N., Houck, M., Eds.; Taylor & Francis, 2010; Chapter 5, pp 590–665.

[5] Virkler, K.; Lednev, I. K. Analysis of body fluids for forensic purposes: From laboratory testing to non-destructive rapid confirmatory identification at a crime scene. *Forensic Science International* **2009**, *188*, 1–17.

[6] Saferstein, R. In *Forensic Science: From the Crime Scene the to Crime Lab*, 1st ed.; Anthony, V., Peyton, T., Kelly, A., Eds.; Pearson Education, Inc., 2009; Chapter 14, pp 457–464.

[7] Harbison, S.; Fleming, R. I. Forensic body fluid identification : state of the art. *Research and Reports in Forensic Medical Science* **2016**, 11–23.

[8] Goldman, E. R.; Mattoussi, H.; Anderson, G. P.; Medintz, I. L.; Mauro, J. M. In *NanoBiotechnology Protocols*, 303rd ed.; Rosenthal, S. J., Wright, D. W., Eds.; 2005; pp 19–34.

[9] Alvarez, M.; Juusola, J.; Ballantyne, J. An mRNA and DNA co-isolation method for forensic casework samples. *Analytical Biochemistry* **2004**, *335*, 289–298.

[10] Virkler, K.; Lednev, I. K. Raman spectroscopy offers great potential for the nondestructive confirmatory identification of body fluids. *Forensic Science International* **2008**, *181*, 1–5.

[11] Granger, R.; Yochum, H.; Granger, J.; Sienerth, K. *Instrumental Analysis*; Oxford University Press, 2017; pp 387–391.

[12] Thomas, J.; Buzzini, P.; Massonnet, G.; Reedy, B.; Roux, C. Raman spectroscopy and the forensic analysis of black/grey and blue cotton fibres: Part 1. Investigation of the effects of varying laser wavelength. *Forensic Science International* **2005**, *152*, 189–197.

[13] Geiman, I.; Leona, M.; Lombardi, J. R. Application of Raman Spectroscopy and Surface-Enhanced Raman Scattering to the Analysis of Synthetic Dyes Found in Ballpoint Pen Inks. *Journal of Forensic Sciences* **2009**, *54*, 947–952.

[14] Hodges, C. M.; Akhavan, J. The use of Fourier Transform Raman spectroscopy in the forensic identification of illicit drugs and explosives. *Spectrochimica Acta Part A: Molecular Spectroscopy* **1990**, *46*, 303–307.

[15] Eliasson, C.; Macleod, N. A.; Matousek, P. Noninvasive detection of concealed liquid explosives using Raman spectroscopy. *Analytical Chemistry* **2007**, *79*, 8185–8189.

[16] De Gelder, J.; Vandenabeele, P.; Govaert, F.; Moens, L. Forensic analysis of automotive paints by Raman spectroscopy. *Journal of Raman Spectroscopy* **2005**, *36*, 1059–1067.

[17] Larkin, P. J. *IR and Raman Spectroscopy: principles and spectral interpretation*; Elsevier Inc., 2011; pp 7–21.

[18] Smith, E.; Dent, G. *Modern Raman Spectroscopy: A Practical Approach*; John and Wiley & Sons, Inc., 2005; pp 1–20, 71–76.

[19] Otto, A.; Mrozek, I.; Grabhorn, H.; Akemann, W. Surface-enhanced Raman scattering. *Journal of Physics: Condensed Matter* **1992**, *4*, 1143–1212.

[20] Rana, V.; Cañamares, M. V.; Kubic, T.; Leona, M.; Lombardi, J. R. Surface-enhanced Raman Spectroscopy for Trace Identification of Controlled Substances: Morphine, Codeine, and Hydrocodone. *Journal of Forensic Sciences* **2011**, *56*, 200–207.

[21] Evanoff, D. D.; Chumanov, G. Synthesis and optical properties of silver nanoparticles and arrays. *ChemPhysChem* **2005**, *6*, 1221–1231.

[22] Evanoff, D. D.; White, R. L.; Chumanov, G. Measuring the Distance Dependence of the Local Electromagnetic Field from Silver Nanoparticles. *The Journal of Physical Chemistry B* **2004**, *108*, 1522–1524.

[23] Sur, U. K. Surface-Enhanced Raman Scattering. *Raman Spectroscopy and Applications* **2017**, *27*, 241–250.

[24] Stiles, P. L.; Dieringer, J. A.; Shah, N. C.; Van Duyne, R. P. Surface-Enhanced Raman Spectroscopy. *Annual Review of Analytical Chemistry* **2008**, *1*, 601–626.

[25] Burleson, M. SERS-Active Nylon Fiber Evidence Swabs For Forensic Applications. Ph.D. thesis, Western Carolina University, 2016.

[26] Brevnov, M. G.; Pawar, H. S.; Mundt, J.; Calandro, L. M.; Furtado, M. R.; Shewale, J. G. Developmental Validation of the PrepFiler? Forensic DNA Extraction Kit for Extraction of Genomic DNA from Biological Samples. *Journal of Forensic Sciences* **2009**, *54*, 599–607.

[27] Yang, W.; Shen, C.; Ji, Q.; An, H.; Wang, J.; Liu, Q.; Zhang, Z. Food storage material silver nanoparticles interfere with DNA replication fidelity and bind with DNA. *Nanotechnology* **2009**, *20*.

[28] Klosky, S.; Woo, L. Solubility of Silver Oxide. *Journal of Physical Chemisty* **1926**, *30*, 1179–1180.

[29] Evanoff, D. D.; Chumanov, G. Size-Controlled Synthesis of Nanoparticles. 1. ”Silver-Only” Aqueous Suspensions via Hydrogen Reduction. *Physical Chemistry* **2004**, *108*, 13948–13956.